Vortex Duality in Higher Dimensions

Beekman, A.J.

Citation

Beekman, A. J. (2011, December 1). *Vortex Duality in Higher Dimensions*. *Casimir PhD Series*. Retrieved from https://hdl.handle.net/1887/18169

Chapter 5

Type-II Mott insulators

In chapter 3 we have seen that the Bose-Mott insulator is in fact a disordered superfluid, where the superfluid vortices have proliferated, and furthermore that the Bose-Mott insulator supports vortices of its own, in the form of lines of supercurrent. This we coined the type-II Bose-Mott insulator. In chapter 4 we have seen how to formulate a relativistic description of Abrikosov vortices in a superconductor, and thus how to wire in electromagnetism. It is now time to combine the acquired knowledge, and to look at vortices in the charged Bose-Mott insulator.

The essence is very much the same as the charge-neutral case, but the outcome is striking: lines of electric current piercing through an otherwise insulating slab of material. These Mott vortex lines contain a quantum of electric current, just as Abrikosov vortices have a magnetic flux quantum. In fact, almost all of the electrodynamic properties of a type-II superconductor are mirrored in the type-II Mott insulator, where "magnetic field" has to be substituted for "electric current".

There are a few notable exceptions to this principle. Firstly, the electric current $J_\mu = \frac{e^*}{\hbar} w_\mu$ is a vector quantity, whereas the magnetic field or rather the Maxwell field strength is a 2-form. As such, the coupling to the vortex world sheet of the current is mathematically different when compared to the magnetic field. The reason for this is easily understood intuitively: the vortex is a line of electric current, which is electric charge in motion. If such a line moves, it is just that the microscopic charges are moving in a different direction than 'straight up'. Compare this to a magnetic field, which in motion generates an electric field. Surely this is a rather different situation.

Secondly, in a superconductor one has the true vacuum where electromagnetic fields are free, and the Meissner state where those fields are expelled. Now the Bose-Mott insulator mimics the Meissner state, yet for electric current instead of magnetic field; the superconductor where current is free mimics the vacuum; but on top of that we still have the real vacuum, and this has no counterpart in superconductivity. Therefore the physical situation is even richer than for type-II superconductors.

In this chapter we will repeat the duality calculation for charged superfluids, that is, a superfluid made out of Cooper pairs. First we will present a short exposition of the realization of such systems in actual materials. Afterwards considerable time will be spent on the nature of the Mott vortex world sheets. Then we collect the relevant physical observables from the equations of motion. All effects are collected in a phase diagram. And lastly, we present a host of possible experimental setups that may be able to identify the vortices in the Mott insulator.

5.1 Charged superfluid–insulator transitions

There are several systems whose properties are principally that of charged bosons, with either weak (superfluid) or strong (insulating) effective interactions. The very well-controlled optical lattice systems mentioned before [50] do not fall into that category as the strong repulsive interaction between charged atoms would dominate the subtle quantum statistical effects.

5.1.1 Arrays of Josephson junctions

Since the 1990s several groups devoted their time to making structures out of superconducting components. Most notable are the arrays of Josephson junctions. These are two-dimensional lattices of superconducting islands with charging energy C which are connected by weak links with Josephson coupling J. These systems are remarkably well described by the Bose-Hubbard model of §2.3, where the boson repulsion U is as the inverse charging energy $1/C$. Good reviews are Refs. [55, 56].

Since they are constructed out of superconducting materials, they are of course electrically charged. As such, they can be probed by electromagnetic means. Also, vortices in the insulating state would be of the kind described

in this chapter.

All in all, this seems like an ideal system to look for type-II behaviour in the Mott insulating state, because the level of control one has in the synthesis of the arrays, and techniques that have already been developed over the past two decades. There is one big caveat however: they have always been restricted to two-dimensional systems. It turns out to be very hard to make truly three-dimensional lattices of this kind. Of course, the two-dimensional version will also have Mott vortices (vortex pancakes), but that prediction is not as striking as the real three-dimensional vortex lines.

5.1.2   Underdoped cuprate superconductors

In 1986 Bednorz and Müller discovered superconductivity in an otherwise very poorly conducting ceramic copper-oxide material up to an unprecedented high temperature. This sparked a true frenzy of research chasing experimentally after new materials with ever higher T_c's and theoretically after the underlying physical mechanism. Up to now, the first endeavour has progressed reasonably well, while the latter has been stuck for a long time. However, these days most scientists in the field would agree that the unconventional properties of the cuprate (and other high-T_c) superconductors lie more in the 'normal' state than in the superconducting one.

The critical temperature T_c below which superconductivity prevails is a function of the chemical doping (adding electron or hole carriers) of the material. The highest T_c is said to be at *optimal doping* (OP). With fewer carriers it is *underdoped* (UD), with more it is *overdoped* (OD). On the overdoped side, the normal state above T_c is much like a regular Fermi liquid (normal metal). But the properties on the underdoped side of the cuprates like $La_{2-x}Sr_xCuO_4$ or $YBa_2Cu_3O_{7-\delta}$ are very peculiar indeed. People find all kinds of electronic ordering [78] like stripes [79, 80], orbital currents [81] and recently also quantum nematics [82–84]. Furthermore a second energy gap (distinct from the superconducting gap) shows up the single-electron spectrum, dubbed the *pseudogap*. See the phase diagram in figure 5.1.

A hypothesis that has many proponents is that in the pseudogap region, electrons do already combine into *preformed* Cooper pairs, which causes the energy gap by the removal of electron states, but the phase fluctuations are too strong to induce long-range phase coherence, such that there is no superconducting order yet [85, 86]. Viewed from the opposite side starting from
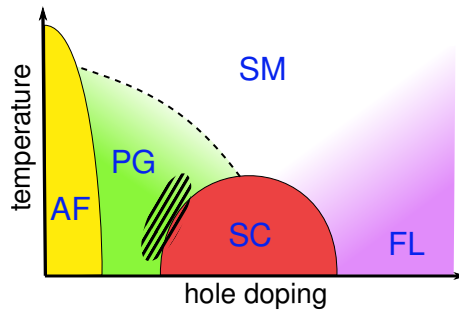
Figure 5.1: Sketch of the generic phase diagram of hole-doped cuprate supercon-
ductors. The only undisputed phases are the antiferromagnetic Mott insulator (AM,
yellow), superconductor (SC, red) and Fermi liquid (FL, purple). Right above the
superconducting dome is a region with electric resistivity that grows linearly with
temperature, and is therefore often referred to as strange metal (SM, white). In
green is shown the pseudogap region (PG), with the appearance of an additional gap
in the single electron response. In is unclear whether there is a phase transition or a
crossover to the strange metal. The hatched area crudely indicates where interesting
electronic ordering is found, and also for instance a large Nernst effect; this is also
the first candidate to look for type-II Mott insulators.

Chapter 5. Type-II Mott insulators

the superconductor: first the phase coherence is destroyed accompanied by the loss of superconductivity, and only at a higher temperature do the Cooper pairs break up. If true, this implies that there is a region in the phase diagram with phase-disordered Cooper pairs, c.q. charged bosons. Therefore this state would actually be a charged Bose-Mott insulator, the topic of this chapter.

This is beneficial in two ways: firstly, this is a suitable testing ground to go and find the type-II Mott insulator and the Mott vortices. These materials have been very well studied, and there are many techniques for both synthesis and experimental characterization. Conversely, if the type-II Mott behaviour were to been found, it would constitute strong evidence for the pseudogap regime as a phase-disordered superconductor.

5.2   Vortex world sheets coupling to supercurrent

In this section we will use physical arguments to determine the correct form of the minimal coupling of the Mott vortices to the dual gauge field and therefore the supercurrent. The only ingredient that we need on top of the discussion in §3.4 is that the supercurrent is now electrically charged, with the correspondence $J_\mu = \frac{e^*}{\hbar} w_\mu$. The full calculation will be performed in the next section; here we only want to illustrate to the reader how to view relativistically the current-carrying vortex, in contrast to the Abrikosov vortices of §4.2.

5.2.1   Limiting to 3+0 and 2+1 dimensions

To obtain the appropriate formulation in the fully relativistic 3+1 dimensional case, it will prove very useful to understand first the special cases of 3+0 and 2+1 dimensions, to both of which the full model must reduce as a lower-dimensional hyperspace cut of the 3+1 dimensional spacetime.

In 3+0 dimensions, the minimal coupling of the dual gauge field b_k, which is now a vector field, to the disorder parameter Φ is straightforward,

$$\mathscr{L}_{\text{min.coup.}} = |(\partial_k - ib_k)\Phi|^2 = |\Phi|^2(\partial_k\phi - b_k)^2. \tag{5.1}$$

In the equations of motion, we then find,

$$\partial_k\phi - b_k = 0, \tag{5.2}$$

and acting on this expression with $\epsilon_{mnk}\partial_n$ leads to,

$$w_m = \epsilon_{mnk}\partial_n b_k = \epsilon_{mnk}\partial_n\partial_k\phi = \mathscr{J}_m^{\mathrm{V}}, \tag{5.3}$$

where the last equality is the definition of the vortex current $\mathscr{J}_m^{\mathrm{V}}$. This expression agrees with the intuition that a vortex line in a Mott insulator is parallel to the electric current $J_m^{\mathrm{EM}} = \frac{e^*}{\hbar}w_m$.

As we mentioned before, the minimal coupling Eq. (3.34),

$$\mathscr{L}_{\mathrm{min.coup.}} = \frac{1}{2}|(\partial_\mu - \mathrm{i}\epsilon_{\mu\|\kappa\lambda}b_{\kappa\lambda})\Phi|^2 \tag{5.4}$$

does not specialize back to back to Eq. (5.1) in 3+0 dimensions.

We need to find another form for the minimal coupling, that satisfies the following conditions,

1. The term in the Lagrangian is equivalent to Eq. (3.23), such that only a single additional degree of freedom arises in the Higgs phase;

2. The equations of motion reduce naturally to the cases of 3+0 and 2+1 dimensions.

The problem of matching the two-form gauge field $b_{\kappa\lambda}$ to the one-form condensate phase mode $\partial_\mu\phi$ is equivalent to matching the two-form vortex world sheet $\mathscr{J}_{\kappa\lambda}^{\mathrm{V}}$ to the one-form supercurrent w_μ. Fortunately, we can fall back to the limiting cases of 2+1 and 3+0 dimensions, representing a dynamic vortex pancake and a static vortex line respectively.

5.2.2 Static vs. dynamic vortex lines

In 3+0 dimensions a vortex line $\mathscr{J}_l^{\mathrm{V}}$ in the Mott insulator is just a static line of electric current $J_l^{\mathrm{EM}} \sim w_l$. Since here the time dimension is absent, the three components of the vortex line correspond to the temporal (density) components of the vortex world sheet $\mathscr{J}_{tl}^{\mathrm{V}}$. Therefore these temporal components of world sheet surface elements correspond to the spatial current $\mathscr{J}_{tl}^{\mathrm{V}} \sim w_l$.

In 2+1 dimensions we have a vortex pancake in the spatial xy-plane, which is therefore represented by a scalar quantity, the charge density w_t. When this vortex pancake moves, its charged vortex core moves, which is equivalent to having an electric current as witnessed by the continuity equation $\partial_t w_t + \partial_k w_k = 0$. Since the vortex pancake can be viewed as a slice through
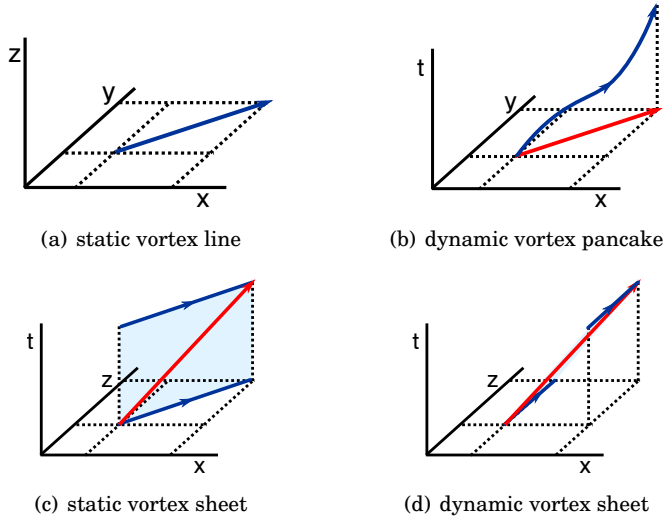
(a) static vortex line   (b) dynamic vortex pancake

(c) static vortex sheet   (d) dynamic vortex sheet

Figure 5.2: (a) Static vortex line in the xy-plane; the current flows through the line. (b) Vortex pancake moving in time (blue). The associated current in the spatial direction is shown in red. (c) Static vortex line in the xz-plane moving straight up in time. (d) A vortex line in the z-direction moving in the x-direction through time. The last two world sheet configurations correspond to the same electromagnetic current (red).

4-dimensional spacetime orthogonal to the third spatial direction l, this suggests that $\mathscr{J}^{\mathrm{V}}_{\kappa l} = \frac{e^*}{\hbar} w_\kappa$.

So here we find electric current as well, but of a different origin: in 3+0 we have a static line *through which* the current is flowing, whereas in 2+1 dimensions the *motion of the vortex itself* causes electric current. Therefore in 3+1 dimensions, we must have both of these contributions.

This is depicted in Figure 5.2. The static vortex line in the xz-plane that moves straight up in time generates the same electric current as a vortex line that is always along the z-direction but moves in the x-direction through time. In other words: the current in the z-direction can originate from the density of vorticity in the z-direction $\mathscr{J}^{\mathrm{V}}_{tz}$; or from lines along x or y that move in the z-direction, represented by $\mathscr{J}^{\mathrm{V}}_{az}$, $a = x, y$. The total current in the z-direction therefore is,

$$w_z \sim \mathscr{J}^{\mathrm{V}}_{tz} + \mathscr{J}^{\mathrm{V}}_{xz} + \mathscr{J}^{\mathrm{V}}_{yz} = \sum_\kappa \mathscr{J}^{\mathrm{V}}_{\kappa z}. \tag{5.5}$$

Now for the charge density[1] w_t, we note that is is an undirected quantity. The charge density does not care in which direction the vortex line is pointing. Therefore the charge density gets contributions from world sheet elements that represent the density of vorticity in all spatial directions, $w_t \sim \sum_\kappa \mathcal{J}^{\mathrm{V}}_{\kappa t}$. Therefore we may conclude that,

$$w_\lambda \sim \sum_\kappa \mathcal{J}^{\mathrm{V}}_{\kappa \lambda}. \tag{5.6}$$

The continuity equation for the electric current $\partial_\lambda w_\lambda = 0$ is satisfied due to the no-monopoles condition of the vortex world sheet $\partial_\lambda \mathcal{J}^{\mathrm{V}}_{\kappa \lambda} = 0$. In the limiting cases of 3+0 or 2+1 dimensions, for each component of the current w_λ there is only a single contribution from the vortex (world) line, and then there is no summation. The 3+1 dimensional vortex world sheet $\mathcal{J}^{\mathrm{V}}_{\kappa \lambda}$ reduces to the special limits of 2+1 and 3+0 dimension as follows. The static vortex line in 3+0 dimensions has only the density components, or $\mathcal{J}^{\mathrm{V}}_l = \mathcal{J}^{\mathrm{V}}_{tl}$. For 2+1 dimensions, we picture a vortex line in the z-direction, and we take a slice in the txy-hyperplane; then $\mathcal{J}^{\mathrm{V}}_\kappa = \mathcal{J}^{\mathrm{V}}_{\kappa z}$.

5.2.3 Minimal coupling by sum over vortex components

We propose the following minimal coupling prescription, that satisfies the above mentioned conditions and results in Eq. (5.6),

$$\mathscr{L}_{\mathrm{min.coup.}} = |(\frac{1}{2}\sum_\alpha \delta_{\alpha\kappa}\partial_\lambda - ib_{\kappa\lambda})\Phi|^2 = |\Phi|^2(\frac{1}{2}\sum_\alpha \delta_{\alpha\kappa}\partial_\lambda\phi - b_{\kappa\lambda})^2. \tag{5.7}$$

This is the form already encountered in Eq. (3.30), and we have now presented the physical reason for this form. If we expand the square, we find,

$$
\begin{aligned}
(\frac{1}{2}\sum_\alpha \delta_{\alpha\kappa}\partial_\lambda\phi - b_{\kappa\lambda})^2 &= \frac{1}{4}\sum_\alpha \delta_{\alpha\kappa}\partial_\lambda\phi \sum_\beta \delta_{\beta\kappa}\partial_\lambda\phi - b_{\kappa\lambda}\sum_\alpha \delta_{\alpha\kappa}\partial_\lambda\phi + b_{\kappa\lambda}^2 \\
&= (\frac{1}{4}\sum_{\alpha\beta} \delta_{\alpha\beta})(\partial_\lambda\phi)^2 + \sum_\alpha \phi\partial_\lambda b_{\alpha\lambda} + b_{\kappa\lambda}^2 \\
&= (\partial_\lambda\phi)^2 + b_{\kappa\lambda}^2 \qquad \text{(Lorenz gauge).}
\end{aligned}
\tag{5.8}
$$

---

[1]Even though the Mott insulator as a whole is electrically neutral, the vortex lines carry current because the Cooper pairs can move freely. Therefore this charge density is just the density of Cooper pairs, which is clearly quantized in units of $e^* = 2e$, and the balancing positive charge is not taken into consideration. The same applies of course in a current-carrying metal wire.

In the second step we have performed partial integration, and in the last step we have enforced the Lorenz gauge condition $\partial_\kappa b_{\kappa\lambda} = 0$. Here we see that this form is indeed equal to that of Eq. (3.23), where $\partial_\lambda \phi$ represents the longitudinal component of w_μ and the three degrees of freedom of $b_{\kappa\lambda}$ remaining after the gauge fix are the transversal ones.

Next, in the equations of motion, we will encounter the term,

$$\frac{\partial \mathscr{L}}{\partial b_{\kappa\lambda}} = \frac{1}{2} \sum_\alpha \delta_{\kappa\alpha} \partial_\lambda \phi - \frac{1}{2} \sum_\alpha \delta_{\lambda\alpha} \partial_\kappa \phi - b_{\kappa\lambda}. \tag{5.9}$$

Acting on this expression with $\epsilon_{\mu\nu\kappa\lambda} \partial_\nu$ leads to,

$$\begin{aligned}
\frac{1}{2} \sum_\kappa \epsilon_{\mu\nu\kappa\lambda} \partial_\nu \partial_\lambda \phi - \frac{1}{2} \sum_\lambda \epsilon_{\mu\nu\kappa\lambda} \partial_\nu \partial_\kappa \phi - \epsilon_{\mu\nu\kappa\lambda} \partial_\nu b_{\kappa\lambda} &= \sum_\kappa \epsilon_{\kappa\mu\nu\lambda} \partial_\nu \partial_\lambda \phi - w_\mu \\
&= \sum_\kappa \mathscr{J}_{\kappa\mu}^{\mathrm{V}} - w_\mu. \tag{5.10}
\end{aligned}$$

This precisely agrees with Eq. (5.6).

There are three details that may raise some concern. Firstly, the expression in Eq. (5.7) is not antisymmetric under the interchange $\kappa \leftrightarrow \lambda$. We could write down a fully antisymmetric form, but that would leads to contractions $\sim \sum_\lambda \partial_\lambda \phi$. We suspect that such terms would fall within the gauge volume or would otherwise be dynamically constrained. But in fact, nothing requires the term to be antisymmetric in the first place. In the relevant quantities, such as the vortex current $\mathscr{J}_{\kappa\lambda}^{\mathrm{V}}$, the antisymmetry follows automatically. The expression in Eq. (5.9) is one example of this.

The next point is that the expression in Eq. (5.7) is not strictly gauge invariant. The gauge transformations for the two-form dual gauge field are Eq. (3.5). The resolution of the alternative form Eq. (3.26) was to explicitly leave the gauge volume out of the minimal coupling. But this expression Eq. (5.7) is to be taken gauge fixed. This is not an actual problem, as the physical field content is dictated by the currents, as in Eq. (3.23). As of yet, we have not found a way to balance the three gauge degrees of freedom of the two-form gauge field with the condensate phase mode. It remains our conviction that the minimal coupling to a vector field is rather special in this regard.

Lastly, as mentioned in §3.4.5, there is as of yet no way to complete the "duality squared" procedure with this form of the minimal coupling. Since we know that the outcome will be fine using the alternate form we leave this

aside, and focus here on the more interesting vortices in the Mott insulator themselves.

5.3 Charged vortex duality

Here we perform the duality transformation of §2.4.7 for 3+1 dimensions. About half of the calculation was already done in §4.3, but we now find it convenient here to work in imaginary time.

5.3.1 Dual superconductor

Then starting with the dimensionless action of the Ginzburg–Landau superconductor Eq. (2.37),

$$S_{\mathrm{E}} = \int \mathrm{d}\tau \mathrm{d}^D x \ -\frac{1}{2g}(\partial_\mu^{\mathrm{ph}}\varphi - A_\mu^{\mathrm{ph}})^2 - \frac{1}{4\mu}F_{\mu\nu}^2, \qquad (5.11)$$

we will end up with the Euclidean version of Eq. (4.36),

$$Z = \int \mathscr{D}J_{\kappa\lambda}^{\mathrm{V}} \mathscr{D}A_\mu \mathscr{F}(A_\mu) \mathscr{D}b_{\kappa\lambda} \mathscr{F}(b_{\kappa\lambda}) \mathrm{e}^{-\int \mathscr{L}_{\mathrm{dual}}}, \qquad (5.12)$$

$$\mathscr{L}_{\mathrm{dual}} = \frac{1}{2}g(\epsilon_{\mu\nu\kappa\lambda}\partial_\nu^{\mathrm{ph}}b_{\kappa\lambda})^2 - b_{\kappa\lambda}J_{\kappa\lambda}^{\mathrm{V}} + \epsilon_{\mu\nu\kappa\lambda}\partial_\nu^{\mathrm{ph}}b_{\kappa\lambda}A_\mu^{\mathrm{ph}} - \frac{1}{4\mu}F_{\mu\nu}^2. \qquad (5.13)$$

Here the coupling constants are,

$$\frac{1}{g} = \frac{Ja}{\hbar c_{\mathrm{ph}}}, \qquad \frac{1}{\mu} = \frac{\hbar a^{D-3}}{\mu_0 c_{\mathrm{ph}} e^{*2}}. \qquad (5.14)$$

The first is always dimensionless, the last is dimensionless if $D = 3$, which is the case we are interested in, and we specialize to 3+1 dimensions from now on.

In these dimensionless units, the charge of the vortex minimal coupling is 1, which was the reason for rescaling to these units in the first place. The action above describes one or several individual (Abrikosov) vortex sources that interact via the mediation of the dual gauge fields $b_{\kappa\lambda}$. These gauge fields are the duality transforms of the original Goldstone modes φ. They remember that the bosons are electrically charged by also coupling to the electromagnetic field A_μ. If one were to integrate out the dual gauge fields, one would find an action of charged vortices that couple to each other non-locally. They would have long-range interactions were it not for the electromagnetic fields, which induce Meissner screening.

5.3.2 Vortex proliferation

This is however not what we are interested in at the moment. We are going to proceed and let the vortex strings proliferate into the 'string foam' as explained in §3.2. The disorder parameter Φ is the 'density of the string foam', and the minimal coupling to the gauge field is dictated by the considerations of §5.2. Thus we find,

$$
\mathscr{L} = \frac{1}{2}g(\epsilon_{\mu\nu\kappa\lambda}\partial_\nu^{\mathrm{ph}}b_{\kappa\lambda})^2 + \epsilon_{\mu\nu\kappa\lambda}\partial_\nu^{\mathrm{ph}}b_{\kappa\lambda}A_\mu^{\mathrm{ph}} - \frac{1}{4\mu}F_{\mu\nu}^2
$$
$$
+ \frac{1}{2}|(\frac{1}{2}\sum_\alpha \delta_{\alpha\kappa}\partial_\lambda - ib_{\kappa\lambda})\Phi|^2 + \frac{\tilde{\alpha}}{2}|\Phi|^2 + \frac{\tilde{\beta}}{4}|\Phi|^4. \tag{5.15}
$$

Here we have added Ginzburg–Landau potential energy terms for the dual order parameter, which we will neglect from now on. If $\tilde{\alpha} < 0$, the dual order parameter obtains an expectation value $\langle\Phi\rangle = \sqrt{\frac{|\tilde{\alpha}|}{\tilde{\beta}}} \equiv \Phi_\infty$. This signals the phase transition to the Bose-Mott insulator, with the Mott gap represented by $|\Phi|^2$.

What we would like to do, similar to the procedure in §3.4.5, is dualize the dual phase field ϕ to a conserved current v_μ, integrate out the smooth part, define the Mott vortex current $\mathscr{J}_{\kappa\lambda}^V = \epsilon_{\kappa\lambda\nu\mu}\partial_\nu\partial_\mu\phi$ and integrate out the current v_μ to find the direct coupling of the Mott vortex current to the supercurrent gauge field $b_{\kappa\lambda}$. However, as mentioned before, I have not been able to find a consistent way of doing it for this form of the minimal coupling. Fortunately, the action (5.15) is sufficient to find the Mott vortex electrodynamics, just as it was for the Abrikosov vortices in chapter 4.

5.4 Phenomenology of Mott vortices

In this section we derive observable quantities of the Bose-Mott insulator and its vortices. This mostly follows the same reasoning as for the regular Ginzburg–Landau model of §2.1, see also e.g. [51, ch.4].

5.4.1 Equations of motion

We calculate the equations of motions by varying Eq. (5.15) with respect to $\bar{\Phi}$, $b_{\kappa\lambda}$ and A_μ.

$$(\frac{1}{2}\sum_\alpha \delta_{\kappa\alpha}\partial_\lambda^{\text{ph}} - \mathrm{i}b_{\kappa\lambda})^2\Phi - \tilde{\alpha}\Phi - \tilde{\beta}|\Phi|^2\Phi = 0, \tag{5.16}$$

$$-g\epsilon_{\kappa\lambda\nu\mu}\partial_\nu^{\text{ph}}w_\mu + |\Phi|^2\Big(\frac{1}{2}\sum_\alpha(\delta_{\kappa\alpha}\partial_\lambda^{\text{ph}}\phi - \delta_{\lambda\alpha}\partial_\kappa^{\text{ph}}\phi) - b_{\kappa\lambda}\Big) = \frac{1}{2}\epsilon_{\kappa\lambda\mu\nu}F_{\mu\nu}^{\text{ph}}, \tag{5.17}$$

$$\frac{1}{\mu}\partial_\mu F_{\mu\nu} = -w_\nu^{\text{ph}}. \tag{5.18}$$

Here we have substituted definitions of $w_\mu = \epsilon_{\mu\nu\kappa\lambda}\partial_\nu^{\text{ph}}b_{\kappa\lambda}$ and $F_{\mu\nu} = \partial_\mu A_\nu - \partial_\nu A_\mu$. The superscripts on $F_{\mu\nu}^{\text{ph}}$ and w_μ^{ph} indicate that those quantities carry a velocity ratio in the temporal components: $F_{tn}^{\text{ph}} = \frac{c}{c_{\text{ph}}}F_{tn}$ and $w_t^{\text{ph}} = \frac{c}{c_{\text{ph}}}w_t$. The dimensionful versions of these equations are,

$$-a^2(\sum_\alpha \delta_{\kappa\alpha}\partial_\lambda^{\text{ph}} - \mathrm{i}\frac{a}{\hbar c_{\text{ph}}}b_{\kappa\lambda})^2\Phi + \tilde{\alpha}\Phi + \tilde{\beta}|\Phi|^2\Phi = 0, \tag{5.19}$$

$$-ga^2\epsilon_{\kappa\lambda\nu\mu}\partial_\nu^{\text{ph}}w_\mu + |\Phi|^2\Big(\frac{1}{2}\sum_\alpha\frac{\hbar c_{\text{ph}}}{a}(\delta_{\kappa\alpha}\partial_\lambda^{\text{ph}}\phi - \delta_{\lambda\alpha}\partial_\kappa^{\text{ph}}\phi) - b_{\kappa\lambda}\Big) = \frac{1}{2}c_{\text{ph}}e^*\epsilon_{\kappa\lambda\mu\nu}F_{\mu\nu}^{\text{ph}}, \tag{5.20}$$

$$\frac{1}{\mu_0}\partial_\mu F_{\mu\nu} = -\frac{e^*}{\hbar}w_\nu^{\text{ph}} = -J_{\text{s}\ \nu}^{\text{ph}}. \tag{5.21}$$

In the last equality we used the definition of the supercurrent $J_\nu^{\text{s}} = \frac{e^*}{\hbar}w_\nu$. Note that the last two equations reduce to the equations of motion for the superconductor in the limit $|\Phi|^2 \to 0$. The last equation is the same with or without the Mott condensate, and just reflects the generation of an electromagnetic field by a current. The second equation is basically the extension of the Meissner screening of the electric current as in Eq. (4.54), but is now sourced by Mott vortices ϕ_{MV}. We are now set to discuss the physical content of these equations.

5.4.2 Maxwell equations

The last equation Eq. (5.21) is clearly the inhomogeneous Maxwell equations for a source term $J_{\text{s}\ \nu}^{\text{ph}}$. This equation carries over from the superconductor, and does not pertain as such to the Mott insulating state. The insulating behaviour is due to the screening of the electric current, which is represented

by the term $\sim |\Phi|^2$. Therefore, Eq. (5.21) is just the vacuum contribution to electric and magnetic fields generated by a current source.

5.4.3 Penetration depth

The dual penetration depth $\tilde{\lambda}$ sets the length scale up to which an electric current penetrates in the Mott insulating region. To find it we act on Eq. (5.20) with $\epsilon_{\rho\sigma\kappa\lambda}\partial_\sigma^{\rm ph}$. Contracting repeated indices, and using $\partial_\rho^{\rm ph} w_\rho = 0$, we find in the dual London limit $|\Phi| = \Phi_\infty$,

$$ga^2(\partial_\mu^{\rm ph})^2 w_\rho - \Phi_\infty^2 w_\rho + c_{\rm ph} e^* \partial_\mu^{\rm ph} F_{\mu\rho}^{\rm ph} = -\Phi_\infty^2 \frac{\hbar c_{\rm ph}}{a} \sum_\kappa \mathscr{J}_{\kappa\rho}^{\rm V}. \tag{5.22}$$

Here we used the definition of the vortex current Eq. (3.33). The interpretation of this equation is as follows: a supercurrent w_ρ can be generated by a vortex source $\mathscr{J}_{\kappa\rho}^{\rm V}$. This current is "dual Meissner screened" by the Mott condensate Φ_∞ as witnessed by the second term; but there is also some electromagnetic screening from the 'backreaction' of the induced electromagnetic field. In order to see this, we would like to substitute Eq. (5.21) in this equation. This is however complicated by the additional factors of $\frac{c}{c_{\rm ph}}$, which will clutter up the full expression. Recall however that this electromagnetic screening originates from the superconductor, and must comply with Eq. (4.54). Thus let us take the simplest case, that of static limit with only stationary flow: all time derivatives set to zero. Then we can use $\partial_m F_{mn} = -\frac{\mu_0 e^*}{\hbar} w_n$, to find in the absence of vortex sources,

$$ga^2 \nabla^2 w_n - \Phi_\infty^2 w_n - \frac{\mu_0 e^{*2} c_{\rm ph}}{\hbar} w_n = 0, \qquad \text{or}$$

$$\nabla^2 w_n - \frac{\hbar \rho_{\rm s}}{c_{\rm ph} m^*} \Phi_\infty^2 w_n - \frac{1}{\lambda^2} w_n = 0 \tag{5.23}$$

Here we substituted $ga^2 = m^* c_{\rm ph}/\hbar\rho_{\rm s}$ (see §2.3.6), and used the definition of the London penetration depth $\lambda^2 = \mu_0 e^{*2} \rho_{\rm s}/m^*$. So we indeed find two contributions to screening of electric current. The first $\sim \Phi_\infty^2$ is due to the Mott insulator, and the second remembers that the system originated from a superconductor. This is actually rather odd: the Meissner screening is due to the fact that the superconductor wants to expel the magnetic field, which is not true for the Mott insulator. However, let us make a crude estimate of

the relative strengths of the screening, by inserting the numerical values,

$$\mu_0 = 4\pi.10^{-7} \approx 10^{-6}\text{N/A}^2, \quad e^* \approx 10^{-19}\text{C}, \quad \hbar \approx 10^{-34}\text{Js}, \quad c_{\text{ph}} \approx \frac{1}{300}c \approx 10^6\text{m/s},$$
(5.24)

we find that the relative strengths are

$$\frac{\text{Mott}}{\text{Meissner}} \approx \frac{\Phi_\infty^2}{\mu_0 e^{*2} c_{\text{ph}}/\hbar} \approx \frac{\Phi_\infty^2}{10^{-6}.10^{-38}.10^6.10^{34}} \approx 10^4 \Phi_\infty^2.$$
(5.25)

Now Φ_∞^2 is dimensionless, but as the order parameter of the Mott condensate it should be surely greater than 1. Therefore the expulsion of electric current due to the Mott term is several orders of magnitude stronger than the Meissner screening, and for all purposes the latter may be ignored, also eliminating our interpretative problem.

Hence the dual penetration depth of electric current in the Mott condensate is $\tilde{\lambda} = \sqrt{\frac{\hbar}{c_{\text{ph}} m^*} \rho_s \Phi_\infty^2}$. It depends on many material parameters. Here, as we often do, we encounter the combination $\rho_s \Phi_\infty^2$, which is the product of the superconducting order parameter and the Mott order parameter. At first, one may think that they should be mutually exclusive, as one has either superconducting order *or* Mott insulating order. However one must realize that the Mott insulator is made out of repelling Cooper pairs: the larger the number of Cooper pairs, as denoted by the superfluid density ρ_s, the stronger the electromagnetic effects such as screening. It is just Φ_∞^2 that signals the existence of the Mott state, whereas the combination $\rho_s \Phi_\infty^2$ is the appropriate Higgs mass.

5.4.4 Coherence length

If in Eq. (5.19) we rescale the dual order parameter Φ by extracting it by its equilibrium value $\Phi_\infty = \sqrt{\frac{|\tilde{\alpha}|}{\tilde{\beta}}}$, so $\Phi = \Phi_\infty \Phi'$, and set $b_{\kappa\lambda}$ to zero which is true deep within the Mott insulator, the equation reduces to,

$$\frac{a^2}{|\tilde{\alpha}|}(\partial_\mu^{\text{ph}})^2 \Phi' + \Phi' - \Phi'^3 = 0.$$
(5.26)

Hence we can define the dual coherence length $\tilde{\xi} = \frac{a}{\sqrt{|\tilde{\alpha}|}}$, which depends on the details of the dual symmetry breaking through the precise value of the Ginzburg–Landau parameter $|\tilde{\alpha}|$.

The coherence length is rather unimportant in this story. We are primarily interested in the type-II regime where vortices can arise, and then $\tilde{\xi}$ is very short, perhaps even near the lattice constant. All the questions we ask of the system are related to longer length scales. In other words, we assume the dual London limit where $|\Phi| = \Phi_\infty$ is constant, and $\tilde{\xi}$ denotes the typical scale over which variations of $|\Phi|$ are important.

5.4.5 Current quantization

Now we come to the most striking prediction: the existence of 'quantized' vortex lines of electric current. The equation (5.20) is just as the regular Ginzburg–Landau equation Eq. (2.5), and we can imagine a closed contour over which the change of the phase ϕ is a multiple of 2π, that is,

$$\oint_{\partial\mathcal{S}} \mathrm{d}x^\mu \partial_\mu \phi = 2\pi N. \tag{5.27}$$

We are free to choose this contour deep within the Mott insulator far away from the vortex line, such that the electric current in suppressed $w_\mu = 0$. Now assume there is no external electromagnetic field $F_{\mu\nu}^{\mathrm{ext}} = 0$, and the induced field is very small as argued in Eq. (5.25). Then Eq. (5.20) reduces to,

$$\frac{1}{2}\sum_\alpha \frac{\hbar c_{\mathrm{ph}}}{a}(\delta_{\kappa\alpha}\partial_\lambda\phi - \delta_{\lambda\alpha}\partial_\kappa\phi) = b_{\kappa\lambda}. \tag{5.28}$$

We restrict our attention to the case $(\kappa\lambda) = tl$, and take the static limit in which all time derivatives are set to zero. Thus we only look at a stationary current flowing through a static vortex line. Then,

$$\frac{\hbar c_{\mathrm{ph}}}{2a}\partial_l\phi = b_{tl}. \tag{5.29}$$

We take the line integral of this equation as in (5.27). On the right-hand side we invoke Stokes' theorem (cf. §2.1.2) to find,

$$\frac{\hbar c_{\mathrm{ph}}}{2a}2\pi N = \frac{\hbar c_{\mathrm{ph}}}{2a}\oint_{\partial\mathcal{S}} \mathrm{d}x^l\ \partial_l\phi = \oint_{\partial\mathcal{S}} \mathrm{d}x^l\ b_{tl} = \int_{\mathcal{S}} \mathrm{d}S_m\ \epsilon_{mnl}\partial_n b_{tl} = \int_{\mathcal{S}} \mathrm{d}S_m\ w_m. \tag{5.30}$$

In the last step we have used the definition of the dual gauge field Eq. (3.4) in the static limit. The right-hand side is the flux of current w_m through the surface $\mathcal{S}$. Since the current is expelled from the Mott insulator, this current

flows through the vortex line. For the electric current I which is the flux of the current density $J_m = \frac{e^*}{\hbar} w_m$, this implies the quantization condition,

$$I_0 = \frac{e^*}{\hbar} \frac{\hbar c_{\mathrm{ph}}}{2a} 2\pi N = \frac{1}{\Phi_0} \sqrt{UJ} 2\pi^2 N. \qquad (5.31)$$

Here $\Phi_0 = h/e^*$ is the (magnetic) flux quantum and we have substituted the microscopic parameters $\sqrt{UJ} = \hbar c_{\mathrm{ph}}/a$ from §2.3.3.

Admittedly, this is no 'true' quantization as the current quantum depends on material parameters. This is however not unexpected, since, contrary to for instance conductivity or magnetic flux, there is no combination of natural constants that results in a unit of electric current. In any case, for a certain material under fixed environmental conditions, the current should penetrate through the Mott insulator in incremental steps of size of the current quantum. From a duality perspective, it is nice that the current quantum is proportional to the inverse of the flux quantum.

If the phase velocity c_{ph} is the same or similar for the Bose-Mott insulator as for the superconductor, then we can make a quick estimate for the $N = 1$ quantum by inserting $c_{\mathrm{ph}} \approx 10^6$m/s and $a = 10^{-10}$m, such that

$$I_0 = \frac{e^* c_{\mathrm{ph}}}{2a} 2\pi \approx 5.10^{-3} \mathrm{A}, \qquad (5.32)$$

which seems rather large at first sight.

5.5   The phase diagram of the type-II Bose-Mott insulator

We shall now collect all acquired knowledge about the type-II Bose-Mott insulator in a phase diagram, figure 5.3. The phase is a function of three, or rather four external parameters. The quantum phase transition from a superconductor to a Bose-Mott insulator is dependent on the coupling constant $g \sim U/J$ (see §§2.3.3, 2.3.7). Next to quantum fluctuations there are thermal fluctuations at any finite temperature T. The phase diagram is presented as is common in the literature of quantum phase transitions: increasing quantum fluctuations on the horizontal axis, and temperature on the vertical axis.

On top of this we can disturb the system by external electromagnetic means. For the superconductor we know that applied magnetic field competes with the superconducting order. And in this chapter we have learned
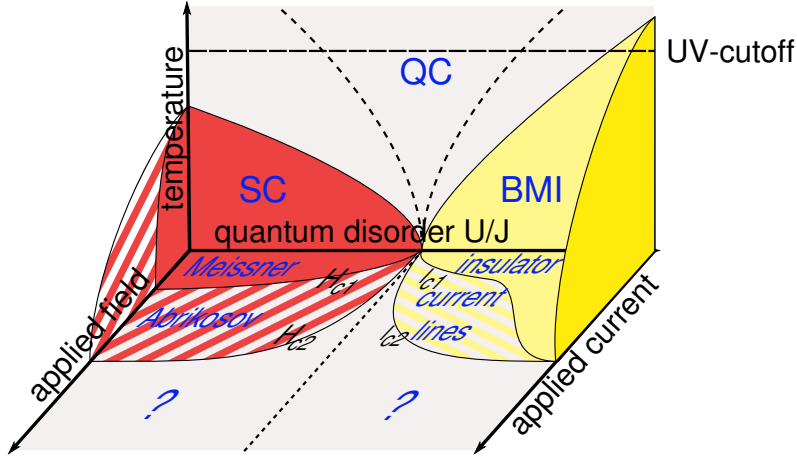
Figure 5.3: Proposed phase diagram of the type-II Bose-Mott insulators. On the horizontal axis is the strength of the quantum fluctuations that disorder the superconductor (SC) into a Bose-Mott insulator (BMI). On the vertical axis is the temperature.

In the plane there is increasing applied magnetic field H for the superconductor, resp. applied electric current I for the Bose-Mott insulator. For both the superconductor and the Bose-Mott insulator at low applied field or current, all of it is expelled by the (dual) Meissner effect. When the first flux or current quantum is generated above the lower critical field H_{c1} or current I_{c1}, the system enters in to a mixed, Abrikosov state. When the applied field or current exceeds the upper critical field H_{c2} or current I_{c2}, all of the superconductivity or insulation order is destroyed. It is unclear what will be the resulting phase at zero temperature (see text).

At finite temperature, we expect the canonical behaviour of quantum phase transitions, with a quantum critical (QC) region right above the quantum critical point. At high temperatures, the superconducting state goes over into the normal state. The Bose-Mott insulator can only originate from a Bose system of Cooper pairs; breaking up the bosons should also lead back to the normal state. When the interactions between the bosons becomes infinitely strong $U \to \infty$, the system will stay insulating. This sets a UV-limit on the applicability of our model.

that the equivalent effects in type-II Mott insulators are due to applied electric current. These two variables are drawn in the plane of the phase diagram, magnetic field for the superconducting side, and electric current for the insulating side.

There a lot going on here, so let us explore the diagram step by step. We will go through to the overly well-known superconductor in some detail, because the same reasonings will be mirrored on the insulating side.

5.5.1 Superconducting side

Surely, the superconductor holds no surprises at all. It should completely reproduce the familiar H–T-diagram found in any textbook. That is, the superconducting order persists below the critical temperature T_c, which is a decreasing function of magnetic field. When, for a particular temperature, the applied field exceeds the so-called *critical field* H_c, superconducting order is completely destroyed, and we end up in the normal state (a metal for conventional superconductors).

In a type-II superconductor, we distinguish the Meissner state below the *lower critical field* H_{c1}, and the Abrikosov state between H_{c1} and the *upper critical field* H_{c2}. The Meissner state is just as for type-I superconductors: a countercurrent will perfectly oppose the applied magnetic field. Above H_{c1}, it is energetically favourable to let magnetic field penetrate through an Abrikosov vortex line. Increasing field will create more and more of these vortices in a triangular lattice. When the applied field is so large that the vortices start to overlap (when they are approximately spaced by the penetration depth λ), superconductivity is destroyed.

In BCS theory, the superconducting gap decreases with temperature until it vanishes at T_c. The gap is proportional to the superfluid density, i.e. the 'strength' of the superconducting condensate. Therefore it is natural that the critical fields H_{c1} and H_{c2} are lower at higher temperatures, since it is easier to perturb the superconducting order.

Similarly, quantum fluctuations can diminish the superconducting order. This whole work is centred around the idea that increasing quantum disorder is just the growth of spontaneous creation and annihilation of vortex–anti-vortex pairs. Therefore increasing quantum fluctuations has the same effect as increasing thermal fluctuations: it is easier to destroy the superconducting condensate, so that the critical applied fields are lower. The situation

for zero temperature and high applied field will be discussed at the end of this section.

5.5.2 Insulating side

The Bose-Mott insulator basically mimics the superconductor, where applied current takes the role of applied magnetic field. Some exceptions are foreseen on simple physical grounds as we proceed.

The point of departure is the no-fluctuations, no-applied current regime, where the system is just a "boring" Bose-Mott insulator. Approaching the quantum phase transition $U/J \to 1$, the bosons repel each other less strongly, such that the dual order parameter $|\Phi|^2$ shrinks, causing the critical temperature or critical current to diminish. The applied electric current is as the applied field for a superconductor: it competes with the established order. At first, all applied current is expelled, showing purely insulating behaviour. But in the type-II regime detailed in this chapter, above the *lower critical current I_{c1}*, vortex lines of current will be created. The current starts to penetrate in multiples of the current quantum I_0, until it is so large that the Mott order is completely destroyed. This point we call the *upper critical current I_{c2}*. It should not be confused with the critical current in a superconductor, which destroys superconducting order by inducing a too high magnetic field.

As opposed to the superconducting side, in the 'atomic' or infinite strong-coupling limit $U/J \to \infty$, there is no way in which the Mott insulating order can be perturbed. As such, at least formally, the insulating behaviour should persist and no current vortex lines can be formed. This could be characterized as the 'type-I' regime of the Mott insulator. Moreover, within the limits of validity of the model, this insulator will not be destroyed at any finite temperature. Therefore we have indicated a UV-cutoff in the phase diagram, above which our model is no longer descriptive. One could imagine for instance that the Cooper pairs will break up across this cut-off, so that there are no charged bosons to begin with.

This all seems quite straightforward, but it is actually profoundly surprising. In the regular XY-model, a 2-dimensional Bose-Mott insulator exists only at zero temperature, and it is destroyed at any finite temperature due to strong fluctuations (see e.g. [87, 88]). On the superfluid side there is still a finite-temperature Kosterlitz–Thouless transition because there the

interactions are logarithmically long-range, but on the insulating side the dual gauge fields are massive. However the 3+1D Mott insulator at finite temperature is in the 4d XY universality class, and reverts basically to the mean-field result as it is at its upper critical dimension. The simple fact that there *is* a finite-temperature phase transition in a Bose-Mott insulator, even though it is just due to a higher dimensionality, is a novelty by itself.

5.5.3   Quantum critical regime

In this work we have not made any calculation at finite temperatures, and all our inferences for that regime stem from established knowledge. Actually, in the quantum disorder–temperature plane without applied field or current, this would just be the standard superconductor–Bose-Mott insulator quantum phase transition. Therefore, we expect a quantum critical point at zero temperature and associated quantum critical regime at finite temperature. The critical behaviour is also not part of this work.

Concurrently, it is not quite clear what happens at zero temperature when the applied field or current grows too large. For the superconductor one may still expect a transition to the normal state. However, the superconductor is destroyed by a large applied field because it induces a very large countercurrent. If the normal state is a Fermi liquid, and the Fermi liquid is intrinsically resistive, any current will immediately generate heat, making the assumption of zero temperature invalid. Similarly, if the 'normal' state is insulating as for instance in the underdoped cuprates, it is also hard to picture how a too large current can go over into insulating behaviour.

The situation is even more clear for the Bose-Mott insulator. Once the current permeating through the dual vortices gets too large, surely all of the insulator is destroyed. The current flowing is actually supercurrent: the vortex cores are locally superconducting as dictated by the duality. Therefore a large applied current should render the type-II Bose-Mott insulator into a superconductor. But the superconductor will be destroyed by a large current itself.

These considerations make us postpone a definite statement on the state of matter at zero temperature and large applied field or current. These regions are therefore indicated by a question mark *?* in the phase diagram.

5.5.4   Application to underdoped cuprates

We shall briefly map this general phase diagram onto the relevant phases of the underdoped cuprates (see figure 5.1). Surely, in real life things work differently than as pictured in the idealized scenario.

In the cuprates the quantum fluctuations are controlled by chemical doping, and it is therefore not possible to tune along the horizontal axis within one material sample. For each sample on the underdoped side, there is a thermal transition from the superconducting to the pseudogap state. But collecting data from several samples, there should also be an effective transition along the horizontal direction, which should therefore be governed by quantum fluctuations. The quantum critical point in the phase diagram of Fig. 5.3 does not appear as such in the cuprates—if at all present, many people believe a quantum critical point to be hidden by the superconducting 'dome', and it is actually related to the transition from the (doped) Mott insulating state to the Fermi liquid at large dopings, and probably of intrinsic fermionic nature.

Still, as we mentioned in §5.1.2, there is evidence for the pseudogap region to be a phase-disordered superconductor, and therefore a Bose-Mott insulator of repelling Cooper pairs. Thus, the transition (at a fixed finite temperature) from the superconductor to the pseudogap should be as the increasing quantum disorder transition of this chapter. Increasing quantum disorder is the increase of the fluctuations in the superconductor phase field. This suggests that the type-II Bose-Mott insulator may be found in the pseudogap region, and close to the phase transition to the superconductor, because there the Mott order parameter should be small, such that the dual penetration depth is large and vortices can be formed. This region is crudely indicated in Fig. 5.1.

5.6   Experimental signatures

In this chapter we have made a prediction for a new state of matter which we named "type-II Bose-Mott insulator". Whereas a regular (Mott) insulator would either completely expel electric current, or would finally permit current through dielectric breakdown like a capacitor, the type-II Mott insulator supports vortex lines of electric current such that it may penetrate at applied current much smaller than what would be required for complete

breakdown. Furthermore, since the current lines form a (dual) Abrikosov lattice, the conductivity is very inhomogeneous.

Here we outline several experimental setups that may verify the existence of such type-II Mott insulating behaviour. Every time we assume that a clever experimentalist would be able to i) find a type-II Bose-Mott insulating material; ii) be able to make the samples as pictured; and iii) have the right experimental probes available and under full control. The experimental setups are sketched in figure 5.4.

5.6.1   The vacua for electric current

Many effects in superconductivity appear at the boundary between the superconductor and empty space. These are both ground states or 'vacua' of their respective Hamiltonians. A magnetic field is free in empty space, but Meissner screened in the superconductor. These effects have to do with the Anderson–Higgs mechanism: photons are free in empty space but obtain a Higgs mass in the superconductor. In this regard, for the magnetic field also metals, dielectrics and so forth are like the vacuum, only with a different light velocity. The screening of photons in a metal is certainly not the Meissner effect, and the photons do not gain a mass even though they interact heavily with the electrons/quasiparticles. Most clearly, a static magnetic field can exist within a metal.

But for electric current, things are really different. We add a third vacuum: the type-II Bose-Mott insulator. As we have seen, electric current is to the Mott insulator as magnetic field is to the superconductor. Continuing the duality reasoning: the superconductor is to the Mott insulator as empty space is to the superconductor. What we mean is: an electric current is free in the superconductor (as long as it does not exceed the critical current) in the sense that a persistent current may run forever. But this current obtains a Higgs mass in the Bose-Mott insulator, just as the magnetic field does in a superconductor (Eq. (5.1.2)).

Conversely, the relation of empty space to the Bose-Mott insulator has no counterpart in the superconductor. As such, the situation is even richer, and more diverse tunnelling and/or junction experiments could be conceptualized. In figure 5.4, yellow is the type-II Mott-insulator, red is superconductor and blue is empty space.

Even more vacua are to be envisaged. Both the Bose-Mott insulator and

dual Meissner effect

(a) MI immersed in SC

(b) MI with SC leads (giant proximity effect)

(c) MI without SC

dual Josephson vortices   **lower critical current**

(d)   Josephson vortex in SC

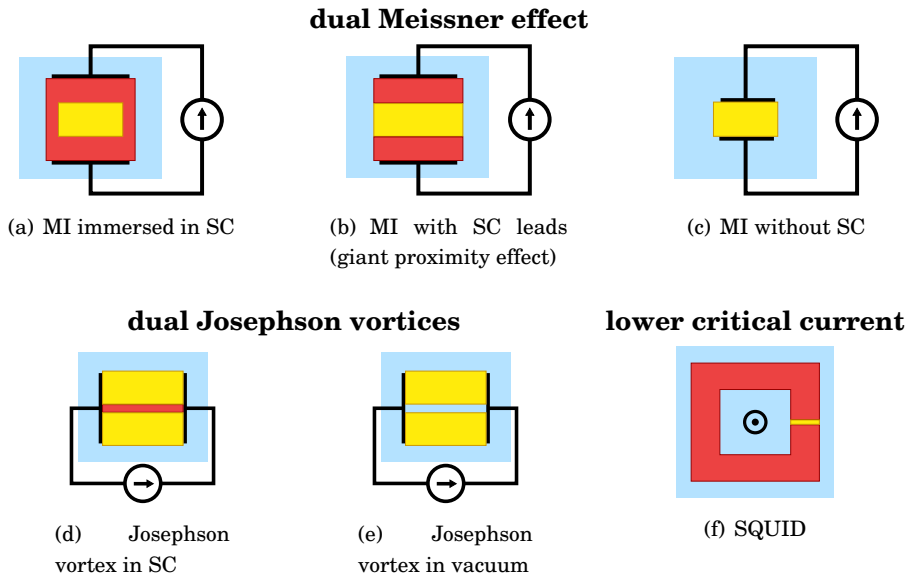(e)   Josephson vortex in vacuum

(f) SQUID

Figure 5.4: Proposed experimental setups. The type-II Bose-Mott insulator (MI) is in yellow; the superconductor (SC) in red; and the empty space/Maxwell vacuum in blue. The circle and arrow represent a current source.

(a) The MI is completely immersed in SC which acts as the "current vacuum". The SC walls should be thin as to curtail the critical current. If current vortex lines will form, the total supercurrent will surpass this critical current. (b) A junction experiment with a thick MI layer between SC leads. This will only succeed if it is not necessary to have the current penetrate bit by bit from the outside, but may force it to form a vortex line from top to bottom immediately. This setup is used in the giant proximity effect (GPE). (c) Capacitor. Perhaps any current bias will cause vortex lines to form, even if it is not supercurrent. Then just MI between normal leads should short-circuit way before dielectric breakdown occurs. (d) Equivalent of Josephson vortices where the vortex line does not form inside MI but within a narrow junction layer of SC. (e) Perhaps the SC vacuum is unnecessary, and a dual Josephson vortex may even form in empty space. (f) SQUID setup in which current bias in increased in very small steps by a perpendicular magnetic field (circle with dot). Current will not flow until the first vortex is formed. This experiment measures the lower critical current.

the superconductor are made out of Cooper pairs, but in a normal metal those pairs are broken up. There simply are more building blocks, especially when making junction geometry setups.

5.6.2   Dual Meissner effect

The Mott insulator wants to expel current as all insulators do. However, when the applied current exceeds the lower critical current I_{c1}, dual vortices will form as lines of supercurrent, such that at least part of the current is permitted to flow through the material. Similar to showing the Meissner effect by measuring the magnetization of a block of superconducting material in the presence of a magnetic field, this dual Meissner effect for current may be demonstrated.

As explained in §5.6.1, the immediate analogue of the superconductor in an applied magnetic field is to immerse a block of type-II Mott insulator in superconducting material. This is because the common understanding is that the magnetic field lines penetrate from the outside to the centre to form the first vortex; similarly angular momentum in a superfluid travels from the outside in to form the first vortex. Now we have electric current which is not supported in the Maxwell vacuum but it is in the superconductor.

Therefore the first thing to try is pictured in Fig. 5.4(a). Current is induced to flow through the superconductor. Since current in a superconductor always flows near the boundary, it must be very narrow where the Mott insulator is immersed, presumably within one penetration depth λ. If the Mott insulator were perfectly insulating, the critical current J_c for this configuration would be limited by the narrow superconducting layers. But if vortices can form, some of the current will flow through the Mott insulator, leading to a much higher critical current.

It could also be that the current vortex lines will form even without superconducting leads, by just forcing regular, not super-, electric current through the Mott insulator. This is pictured in Fig. 5.4(c), and is in fact a capacitor. For a true insulator, current will only flow after dielectric breakdown, which only happens for really large currents. But if vortices form, that will happen at much lower current biases. There may be additional interface effects such as Andreev reflection, but it is our conviction that any form of electric current bias should suffice.

It may be that the vortices will only form if the applied current is a su-

percurrent. Then the leads should be made out of superconductor, as in Fig. 5.4(b). The signature will be the same: no current will flow for a good insulator, but current will soon flow for a type-II Mott insulator. In fact, this may have already been measured, related to the so-called giant proximity effect (GPE). Right after the high-temperature superconductors were discovered, people made junction setups to study their properties. An interesting type of junction is to have a superconductor of lower T_c sandwiched between two layers of material with higher T_c, and measure at a temperature right in between [89]. The question is whether the leads will induce superconductivity in the middle layer which is above its T_c. Surprisingly, a supercurrent was observed even in very thick layers, which does not conform to the regular Josephson effect, that is ultimately caused by the overlap of exponentially decaying wave functions. Even though there was some doubt related to the presence impurities, the final word seem to be that the effect is real [90]. It is also unexplained up to this day.

There is a proposal by Marchand *et al.* [91] that suggests that the phase rigidity of the superconducting leads prevents vortices to unbind in the middle layer, thus retaining the superconductivity even above T_c, not unlike the theme of this thesis. However, we suggest another mechanism: the formation of vortex lines of electric current. This automatically enables the middle layer to be very thick, because the energy cost of a vortex line grows as the length of the line, where as all other mechanisms affect the whole layer homogeneously, scaling as the volume. The telltale difference between our proposal and the earlier one, is that the vortex lines will show as an inhomogeneous distribution of conductivity, as opposed to homogeneous.

5.6.3 Dual Josephson vortices

In §4.4.3 we mentioned that, in superconductors, there can also be vortices in Josephson junctions, which are quantized but do no have a normal core and no core energy. This situation may be mimicked in the type-II Mott insulator. The influence of the Mott condensate will stray just beyond the edge of the material, so that in narrow gaps also vortices may arise. They are parallel to the edge of the Mott insulator.

Following the argument in §5.6.1 the immediate analogue of the Josephson vortex would be to have a very thin layer of superconductor between two pieces of type-II Mott insulator as in Fig. 5.4(d). Setting a current bias along

the layer should cause the formation of vortices, manifested as a line of electric current. Of course, current flowing through a superconductor is nothing special, so this effect may not exist, or it may be very hard to detect. Still, the vortices are quantized, and therefore different in nature from regular supercurrent.

Another thing to try is to leave out the superconductor, and see whether a vortex can form under the influence of the Mott condensate wave function in the Maxwell vacuum (Fig. 5.4(e)). It is however hard to imagine how electric current would flow through empty space, and this is definitely not the first place to look for this effect. Other vacua such as a normal metal may also be interesting.

5.6.4 Lower critical current

Instead of trying to see the vortices directly, one could also attempt to determine when the first vortex is formed, that is: what is the value of the lower critical current I_{c1}? One advantage is that current is measurable to very high precision. We propose a superconducting quantum interference device (SQUID) setup as in figure 5.4(f). The (Josephson) junction in the SQUID is now made of type-II Mott insulator.

Applying a magnetic field perpendicular to the loop as indicated will induce a (persistent) current in the superconductor. Related to the phenomenon of flux quantization (§2.1.2), the magnetic field will only penetrate through the inner area when the current is actually allowed to flow. Reading out the amount of field that does get through, for instance by another SQUID, will tell how much current is flowing trough the loop. We envisage that, while increasing applied magnetic field, at first no current will flow until suddenly the first dual vortex will form and current does start to flow. The point of this jump is precisely the lower critical current I_{c1}. This should continue in a stepwise manner. Not only will this quantitatively determine the value of this parameter, but the sudden jump and ladder pattern are also qualitatively different from regular Josephson junctions.

5.6.5 Inhomogeneous conductivity

In many of the proposed setups in figure 5.4, the type-II behaviour of the Bose-Mott insulator would show in the inhomogeneity of the conductivity.

The typical length scale is the lattice spacing of the dual Abrikosov lattice, which depends the dual penetration depth and the amount of vortices related to the magnitude of the applied current and the size of the current quantum I_0. These parameters in turn depend on the "strength" of the Mott condensate Φ_∞^2, which varies from material to material and presumably also with temperature. This should be calculated or measured on an individual basis. The inhomogeneity itself is however a strong qualitative prediction.

Another problem is that the dual penetration depth $\tilde{\lambda}$ may typically be quite large (see §5.4.3). Presumably, following intuition from regular Abrikosov vortex physics, this would imply that the vortex lines reside quite deep below the edge of the Mott insulator, and all surface sensitive techniques would suffer from this complication.

Leaving these matters aside, there are several techniques that could measure the inhomogeneous conductivity. They should i) have high spatial resolution to see the current lines and the insulating regions in between; ii) have high conductivity resolution to measure the possibly low value of the current quantum I_0; and iii) be able to operate at temperatures low enough that the quantum phase transition dominates thermal fluctuations.

Scanning tunnelling spectroscopy (**STS**) is a very sensitive technique with extremely high spatial resolution. However it cannot probe further than several lattice spacings below the surface. Microwave Impedance Microscopy (**MIM**) directly measures the conductivity and up to 100nm resolution, but suffers the same surface limitations. Low energy electron microscopy (**LEEM**) measures the local electric field non-invasively, and for insulators should be able to do so up to a reasonable depth, and with high spatial resolution. A current problem is to cool the samples to a low enough temperature.

In the appendix 5.A we calculate the conductivity for both the superconducting and the Bose-Mott insulating phases.

5.6.6   Foreseeable complications

There are many possible complications in all of these proposals that may spoil a clean signature of the vortex current lines. It could be that the numbers simply do not work out. The current quantum I_0 seems rather large (§5.4.5), so that there will only be a few vortices deep below the surface. Or, the applied current necessary to induce the first vortex may exceed the

superconductor critical current density J_c.

More importantly, most Mott insulators such as the underdoped cuprates are in fact poor insulators, meaning there will always be leak currents. This can be understood by considering figure 2.3: each excitation of the Mott insulator above the ground state immediately leads to free current carriers. As soon as the doublon and holon are formed, there is no further energy penalty for their hopping around. Therefore any experiment that relies on the distinction between insulating and conducting behaviour, and in particular the lower critical current setup of Fig. 5.4(f), has to deal with this drawback.

But the primary important effect to be expected is the strong pinning of the vortices. It is well known that the cuprates are in the 'dirty' limit where the coherence length is really short. We expect the same to hold for the Mott vortices. An Abrikosov vortex lattice can only exist because of pinning forces, since vortices in motion dissipate energy, and any fluctuation will cause such motion in an unpinned lattice. Indeed, the limiting factor in making high-field superconducting magnet coils is the ability to pin the vortices.

The pinning occurs on so-called pinning centres (impurities or defects), which are distributed unevenly throughout the material. Therefore the vortices follow the pinning centres rather than the vortex lattice, and the lines will most often not really be straight. These effects cause a large deviation from the idealized case. We expect similar behaviour for the Mott vortices. It may cause the vortex state to become 'glassy' and may in particular obscure the transition from the purely insulating to the vortex lattice state under applied current (at J_{c1}). Still, the strong non-linearity in the I–V characteristic should distinguish the type-II Mott insulator from a regular (doped) Mott insulator.

In all of our considerations, we have assumed the dual London limit $|\Phi|(x) = \Phi_\infty$ (no amplitude fluctuations). This should be good in the extreme type-II limit, but since this is all unexplored territory, one should keep a keen eye on a less robust condensate, which may have more obfuscated signatures.

5.7 Summary

We predict a new state of matter called "type-II Bose-Mott insulator". Just as in a type-II superconductor the Meissner effect expels magnetic field but

permits it in the form of quantized vortex flux lines, this material normally expels electric current but permits it in the form of quantized vortex current lines. The current quantum is not fundamental, but depends on system-specific parameters. Otherwise, almost all the properties of type-II super-conductors are mirrored, where magnetic field is to be replaced by electric current. All these features are collected in a new phase diagram (Fig. 5.3).

The current vortex lines may be found in cold atoms in optical lattices, ar-rays of Josephson junctions, but moreover in the pseudogap phase of under-doped cuprates, which are in this context fluctuating Bose-Mott insulators of incoherent Cooper pairs. We have proposed several experiments that may see the current lines (Fig. 5.4). If the type-II Mott behaviour is confirmed, this would be strong evidence of the pseudogap region as a phase-disordered superconductor.

There may be many ways in which this idealized picture can be compli-cated in nature. But since the study of Abrikosov vortices is over 50 years old and still going strong, we believe that with time the current vortex lines will show themselves just as clearly as their superconductor siblings.

5.A   The conductivity of the superconductor and Bose-Mott insulator

Here we calculate the conductivity from the quantum partition sum as the response to an applied electric field. The conductivity σ in imaginary time τ is defined as,

$$\langle j_a(\mathbf{x}, \tau) \rangle = \int \mathrm{d}^D \tilde{x} \mathrm{d}\tilde{\tau} \; \sigma_{ab}(\mathbf{x} - \tilde{\mathbf{x}}, \tau - \tilde{\tau}) E_b(\tilde{\mathbf{x}}, \tilde{\tau}). \tag{5.33}$$

Here a and b are spatial vector indices; $\langle \ldots \rangle$ denotes expectation value. This equation defines the conductivity per spacetime volume, which has units of $\frac{\mathrm{C}^2}{\mathrm{Jsm}^{D-2}} \frac{1}{\mathrm{m}^D \mathrm{s}}$. The volume-integrated conductivity is related to the conductance as $g = \sigma A/l$ in D=3, where A is the area of the conductor, and l its length. This explains the factor $1/\mathrm{m}^{D-2}$ in the previous expression. It is the conductance which has the same units in any dimensions. The quantum of conductance, which features for example in the quantum Hall effect, is $\frac{\mathrm{e}^2}{\mathrm{h}}$.

The electric field can be expressed in terms of electromagnetic potentials,

$$\mathbf{E}(\mathbf{x}, t) = -\nabla V(\mathbf{x}, t) - \partial_t \mathbf{A}(\mathbf{x}, t). \tag{5.34}$$

In our calculation, we will take the functional derivative of this expression with respect to A_a, with a spatial only. Therefore, we will disregard the term $\sim V$, since it will drop out anyway. When going to imaginary time $t \to i\tau$, (5.34) will go over to,

$$\mathbf{E}(\mathbf{x}, \tau) = i\partial_\tau \mathbf{A}(\mathbf{x}, \tau). \tag{5.35}$$

Substituting this expression in (5.33), performing a partial integration, and taking the functional derivative on both sides gives,

$$\frac{\delta}{\delta A_c(y, \tau_y)} \langle j_a(\mathbf{x}, \tau) \rangle = \frac{\delta}{\delta A_c(y, \tau_y)} \int d^D \tilde{x} d\tilde{\tau} \left(-i\partial_{\tilde{\tau}} \sigma_{ab}(\mathbf{x} - \tilde{\mathbf{x}}, \tau - \tilde{\tau}) \right) A_b(\tilde{\mathbf{x}}, \tilde{\tau})$$

$$= \int d^D \tilde{x} d\tilde{\tau} \left(i\partial_\tau \sigma_{ab}(\mathbf{x} - \tilde{\mathbf{x}}, \tau - \tilde{\tau}) \right) \delta_{bc} \delta(\tilde{x} - y)$$

$$= i\partial_\tau \sigma_{ac}(\mathbf{x} - \mathbf{y}, \tau - \tau_y). \tag{5.36}$$

We can define the Fourier transform of the conductivity in terms of Matsubara frequencies ω_n and wave vectors $\mathbf{k}$ as follows,

$$\sigma_{ab}(\mathbf{k}, i\omega_n) = \int d^D \tilde{x} d\tilde{\tau} \, e^{-i\mathbf{k}\cdot\tilde{\mathbf{x}}} e^{-i\omega_n \tilde{\tau}} \sigma_{ab}(\tilde{\mathbf{x}}, \tilde{\tau}) = \int d^d \tilde{x} \, e^{-ik\cdot\tilde{x}} \sigma_{ab}(\tilde{x}). \tag{5.37}$$

To get to the result of (5.36), multiply by the frequency,

$$-\omega_n \sigma_{ab}(\mathbf{k}, i\omega_n) = \int d^d \tilde{x} \left(-\omega_n e^{-ik\cdot\tilde{x}} \right) \sigma_{ab}(\tilde{x}) = \int d^d \tilde{x} \left(-i\partial_{\tilde{\tau}} e^{-ik\cdot\tilde{x}} \right) \sigma_{ab}(\tilde{x})$$

$$= \int d^d \tilde{x} \, e^{-ik\cdot\tilde{x}} \left(+i\partial_{\tilde{\tau}} \sigma_{ab}(\tilde{x}) \right). \tag{5.38}$$

Now substituting $\tilde{x} = x - y$ and noticing that $\partial_\tau f(\tau) = \partial_\tau f(\tau - \tau_y)$, we have indeed derived the Fourier transform of (5.36).

Now the current can be retrieved from the generating functional Z,

$$Z = \int \mathscr{D}\{\text{fields}\} \exp\left(-\frac{1}{\hbar} S_E \right), \tag{5.39}$$

where S_E is the Euclidean action. It is,

$$\langle j_a(x) \rangle = -\hbar \frac{1}{Z[0]} \frac{\delta}{\delta A_a(x)} Z[A]. \tag{5.40}$$

Indeed, when one takes the action of a Ginzburg–Landau superconductor Eq. (2.34),

$$S_E = \int d^D x d\tau \, -\frac{\hbar^2}{2m^*} \rho_s \left(\partial_\mu^{\text{ph}} \phi(x) - \frac{e^*}{\hbar} A_\mu^{\text{ph}}(x) \right)^2, \tag{5.41}$$

one finds

$$\langle j_a(x)\rangle = -\hbar(-\frac{1}{\hbar})(-\frac{\hbar^2}{m^*}\rho_s)(-\frac{e*}{\hbar})\bigl(\nabla_a\phi(x) - \frac{e^*}{\hbar}A_a(x)\bigr)$$

$$= \frac{e^*\hbar}{m^*}|\Psi|^2\bigl(\nabla_a\phi(x) - \frac{e^*}{\hbar}A_a(x)\bigr), \tag{5.42}$$

which agrees with Eq. (2.7).

Now from (5.40), (5.38) and (5.36) we find,

$$\omega_n\sigma_{ab}(\mathbf{k}, \mathrm{i}\omega_n) = \int \mathrm{d}^d(x-y)\,\mathrm{e}^{-\mathrm{i}k(x-y)}\frac{\hbar}{Z[0]}\frac{\delta}{\delta A_b(y)}\frac{\delta}{\delta A_a(x)}Z[A]\Big|_{A=0}. \tag{5.43}$$

The restriction $A = 0$ is taken, because we want to know the *linear* response of the (electron) system; when keeping A around, one also incorporates non-linear contributions.

5.A.1   Superconductor

We have derived the Euclidean action from the charged superfluid in (2.34),

$$S_{\mathrm{E}} = \int \mathrm{d}^D x\mathrm{d}\tau \; -\frac{\hbar^2}{2m^*}\rho_s(\partial_\mu^{\mathrm{ph}}\phi - \frac{e^*}{\hbar}A_\mu^{\mathrm{ph}})^2. \tag{5.44}$$

We also need to include the Maxwell term, which we will treat in the next section.

The temporal components involve a speed, but those components play no role in this calculation. Using this action in the generating functional, we find,

$$\omega_n\sigma_{ab}(\mathbf{k}, \mathrm{i}\omega_n)$$

$$= \int \mathrm{d}(x-y)\mathrm{e}^{-\mathrm{i}k(x-y)}\frac{\hbar}{Z[0]}\frac{\delta}{\delta A_c(y)}(-\frac{1}{\hbar})(-\frac{\hbar^2}{m^*}\rho_s)(-\frac{e^*}{\hbar})\bigl(\nabla_a\phi(x) - \frac{e^*}{\hbar}A_a(x)\bigr)Z[A]$$

$$= \int \mathrm{d}(x-y)\mathrm{e}^{-\mathrm{i}k(x-y)}\Bigl[\frac{e^{*2}}{m^*}\rho_s\delta_{ac}\delta(x-y) + \frac{e^{*2}}{m^{*2}}\rho_s^2\hbar\langle\nabla_a\phi(x)\nabla_b\phi(y)\rangle\Bigr]. \tag{5.45}$$

In the last term appears the velocity–velocity correlation function. This can be easily extracted from the generating functional in the Lorenz or the Coulomb gauge, where the photon fields decouple from the phase velocity $\nabla\phi$, and can be disregarded for this calculation. Adding an external source $\mathscr{J}_\mu$, the action to consider is,

$$S_{\mathrm{E}} = \int \mathrm{d}^D x\mathrm{d}\tau \; -\frac{\hbar^2}{2m^*}\rho_s\frac{1}{2}(\partial_\mu^{\mathrm{ph}}\phi)^2 + \mathscr{J}_\mu\partial_\mu^{\mathrm{ph}}\phi. \tag{5.46}$$

Then,

$$\frac{\hbar^2}{Z[0]}\frac{\delta}{\delta\,\mathscr{J}_b(y)}\frac{\delta}{\delta\,\mathscr{J}_a(x)}Z[\mathscr{J}]\big|_{\mathscr{J}=0} = \frac{1}{Z[0]}\int \mathscr{D}\phi\;\nabla_a\phi(x)\nabla_b\phi(y)\mathrm{e}^{-1/\hbar S_\mathrm{E}}$$

$$= \langle\nabla_a\phi(x)\nabla_b\phi(y)\rangle. \tag{5.47}$$

Next, we complete the square in (5.46) and integrate out the phase field to find,

$$S_\mathrm{E} = \int \mathrm{d}^D x\mathrm{d}\tau\;\frac{\hbar^2}{2m^*}\rho_\mathrm{s}\phi(\partial_\mathrm{ph}^2)\big(\phi-2\frac{1}{\frac{\hbar^2}{m^*}\rho_\mathrm{s}\partial_\mathrm{ph}^2}\partial_\mu^\mathrm{ph}\mathscr{J}_\mu\big)$$

$$= \int \mathrm{d}^D x\mathrm{d}\tau\;-\frac{1}{2}\frac{m^*}{\hbar^2\rho_\mathrm{s}}\partial_\mu^\mathrm{ph}\mathscr{J}_\mu\frac{1}{\partial_\mathrm{ph}^2}\partial_\nu^\mathrm{ph}\mathscr{J}_\nu$$

$$= \int \mathrm{d}^D x\mathrm{d}\tau\,\mathrm{d}^d k\,\mathrm{d}^d k'\;\frac{1}{2}\frac{m^*}{\hbar^2\rho_\mathrm{s}}\mathscr{J}_\mu(k')\mathrm{e}^{ik'x}\frac{\partial_\mu^\mathrm{ph}\partial_\nu^\mathrm{ph}}{\partial_\mathrm{ph}^2}\mathrm{e}^{ikx}\mathscr{J}_\nu(k)$$

$$= \int \mathrm{d}^4 k\;\frac{1}{2}\frac{m^*}{\hbar^2\rho_\mathrm{s}}\mathscr{J}_\mu(-k)\frac{k_\mu^\mathrm{ph}k_\nu^\mathrm{ph}}{k_\mathrm{ph}^2}\mathscr{J}_\nu(k). \tag{5.48}$$

Now, by definition,

$$\frac{\delta}{\delta\,\mathscr{J}_a(x)}\mathscr{J}_b(y) = \delta_{ab}\delta^{D+1}(y-x) = \delta_{ab}\int \mathrm{d}^{D+1}k\;\mathrm{e}^{ik(y-x)}. \tag{5.49}$$

Expressing $\mathscr{J}_b(y)$ in Fourier decomposition, one finds,

$$\frac{\delta}{\delta\,\mathscr{J}_a(x)}\mathscr{J}_b(y) = \frac{\delta}{\delta\,\mathscr{J}_a(x)}\int \mathrm{d}^{D+1}k\;\mathrm{e}^{iky}\,\mathscr{J}_b(k) = \int \mathrm{d}^{D+1}k\;\mathrm{e}^{iky}\big[\frac{\delta}{\delta\,\mathscr{J}_a(x)}\mathscr{J}_b(k)\big]. \tag{5.50}$$

Comparing these two equations, one concludes,

$$\frac{\delta}{\delta\,\mathscr{J}_a(x)}\mathscr{J}_b(k) = \delta_{ab}\mathrm{e}^{-ikx}. \tag{5.51}$$

Now we can evaluate the velocity–velocity correlation function:

$$\langle\nabla_a\phi(x)\nabla_b\phi(y)\rangle = \frac{\hbar^2}{Z[0]}\frac{\delta}{\delta\,\mathscr{J}_b(y)}\frac{\delta}{\delta\,\mathscr{J}_a(x)}\mathrm{e}^{\frac{-1}{\hbar}\frac{1}{2}\frac{m^*}{\hbar^2\rho_\mathrm{s}}\int \mathrm{d}^d k\;\mathscr{J}_\mu(-k)\frac{k_\mu^\mathrm{ph}k_\nu^\mathrm{ph}}{k_\mathrm{ph}^2}\mathscr{J}_\nu(k)}$$

$$= \frac{1}{Z[0]}\frac{\delta}{\delta\,\mathscr{J}_b(y)}\frac{-m^*}{\hbar\rho_\mathrm{s}}\int \mathrm{d}^d k\;\mathrm{e}^{ikx}\frac{k_a k_\nu^\mathrm{ph}}{k_\mathrm{ph}^2}\mathscr{J}_\nu(k)Z[\mathscr{J}]$$

$$= \frac{-m^*}{\hbar\rho_\mathrm{s}}\int \mathrm{d}^d k\;\mathrm{e}^{ik(x-y)}\frac{k_a k_b}{k_\mathrm{ph}^2}. \tag{5.52}$$

Inserting this into (5.45) one finds,

$$\omega_n \sigma_{ab}(\mathbf{k}, i\omega_n) = \int d(x-y) e^{-ik(x-y)} \frac{e^{*2}}{m^*} \rho_s \left[\delta_{ac}\delta(x-y) + \int d^d k' \, e^{ik'(x-y)} \frac{k'_a k'_b}{k'^2_{\text{ph}}} \right]$$

$$= \frac{e^{*2}}{m^*} \rho_s \left[\delta_{ab} - \frac{k_a k_b}{\frac{1}{c^2_{\text{ph}}}\omega_n^2 + \mathbf{k}^2} \right]. \tag{5.53}$$

Now we analytically continue to real time $i\omega_n \to \omega + i\eta$ and invoke the Sokhostsky formula,

$$\lim_{\eta \to 0} \frac{1}{\omega + i\eta} = P\left(\frac{1}{\omega}\right) - i\pi\delta(\omega). \tag{5.54}$$

we finally obtain,

$$\text{Re}\left[\sigma_{ab}(\mathbf{k}, \omega)\right] = \frac{e^{*2}}{m^*} \rho_s \pi \delta(\omega) \left[\delta_{ab} - \frac{k_a k_b}{-\frac{1}{c^2_{\text{ph}}}\omega^2 + \mathbf{k}^2 - i\eta \, \text{sgn}(\omega)} \right]. \tag{5.55}$$

We are especially interested in the zero-momentum conductivity. Taking the limit $\mathbf{k} \to 0$ with ω still finite the complex conductivity reads,

$$\sigma_{ab}(\mathbf{k}=0, \omega) = \frac{e^{*2}}{m^*} \rho_s \delta_{ab} \left(\pi\delta(\omega) - i\frac{1}{\omega} \right). \tag{5.56}$$

This agrees for the conductivity derived from the two-fluid Drude model, with the normal component vanishing, see e.g. [51, eq. 2.44]. The real part of the electric conductivity is peaked at zero frequency, this is the DC conductivity. The imaginary part has the standard form $\sim \frac{1}{\omega}$, valid at non-zero frequencies. It can also be found from invoking the Kramers–Krönig relation. Furthermore it is only valid for frequencies corresponding to energies below the gap; for higher energies pair-breaking events have to be taken into account as well, like in the Mattis–Bardeen model. Since we are deep within the superconductor $\rho_s \gg 1$, the approximation is valid for a large range of frequencies.

5.A.2 Vacuum conductivity

If there is a need to include the Maxwell term, one can derive its conductivity contribution as follows,

$$
\begin{aligned}
S_{\mathrm{E,MW}} &= \int \mathrm{d}\tau \mathrm{d}^D x \, \frac{-1}{4\mu_0} (\partial_\mu^c A_\nu - \partial_\nu^c A_\mu)^2 \\
&= \int \mathrm{d}\tau \mathrm{d}^D x \, \frac{1}{2\mu_0} A_\mu \big((\partial^c)^2 \delta_{\mu\nu} - \partial_\mu^c \partial_\nu^c \big) A_\nu \\
&= \int \mathrm{d}\omega_n \mathrm{d}^D k \, \frac{-1}{2\mu_0} A_\mu(-k) \big((k^c)^2 \delta_{\mu\nu} - k_\mu^c k_\nu^c \big) A_\nu(k).
\end{aligned} \tag{5.57}
$$

Using this expression in the partition function, we find from (5.43),

$$
\begin{aligned}
\omega_n \sigma_{ab}(\mathbf{k}, \mathrm{i}\omega_n) &= \int \mathrm{d}(x - y) \mathrm{e}^{-\mathrm{i}k(x-y)} \frac{\hbar}{Z[0]} \frac{\delta}{\delta A_b(y)} \\
&\qquad \frac{1}{\mu_0 \hbar} \int \mathrm{d}\tilde{k} \mathrm{e}^{\mathrm{i}\tilde{k}x} \big((\tilde{k}^c)^2 \delta_{a\nu} - \tilde{k}_a^c \tilde{k}_\nu^c \big) A_\nu(k) Z[A] \\
&= \int \mathrm{d}(x - y) \mathrm{d}k \, \mathrm{e}^{-\mathrm{i}k(x-y) + \mathrm{i}\tilde{k}(x-y)} \frac{1}{\mu_0} \big((\tilde{k}^c)^2 \delta_{ab} - \tilde{k}_a^c \tilde{k}_b^c \big) \\
&= \frac{1}{\mu_0} \big((k^c)^2 \delta_{ab} - k_a^c k_b^c \big) = \frac{1}{\mu_0} \big((\frac{1}{c^2} \omega_n^2 + \mathbf{k}^2) \delta_{ab} - \mathbf{k}_a \mathbf{k}_b \big).
\end{aligned} \tag{5.58}
$$

By continuation to real time one finds,

$$
\sigma_{ab}(\mathbf{k}, \omega) = \mathrm{i} \frac{1}{\mu_0} \frac{1}{\omega + \mathrm{i}\eta} \big((-\frac{1}{c^2} \omega^2 + \mathbf{k}^2) \delta_{ab} - \mathbf{k}_a \mathbf{k}_b \big). \tag{5.59}
$$

In the limit $\mathbf{k} \to 0$ this reduces to, using (5.54),

$$
\sigma_{ab}(\omega) = \varepsilon_0 \delta_{ab} \big(\mathrm{i}\omega + \pi \delta(\omega) \omega^2 \big). \tag{5.60}
$$

Clearly the second term vanishes for all ω, so the conductivity is purely imaginary, and $\sigma(\omega) = -\mathrm{i}\varepsilon_0 \omega$. This agrees with simple inspection of the Ampère–Maxwell law for $\mathbf{k} \to 0$,

$$
0 = \frac{1}{\mu_0} \mathrm{i}\mathbf{k} \times \mathbf{B} \to \frac{1}{\mu_0} \nabla \times \mathbf{B} = \mathbf{J} + \varepsilon_0 \partial_t \mathbf{E} \to \mathbf{J} + \mathrm{i}\varepsilon_0 \omega \mathbf{E} \equiv \mathbf{J} - \sigma(\omega) \mathbf{E}. \tag{5.61}
$$

The last step is the definition of the conductivity σ [cf. Eq. (5.33)].

5.A.3 Superconductor from dimensionless variables

For the sequel, it will be useful to repeat the calculation employing dimensionless variables as much as possible. First, we need to define the functional derivative. Take a dimensionless field $f(x)$ which is a function of the

dimensionful coordinate x_μ. Then the functional derivative is

$$\frac{\delta}{\delta f(x)} f(y) = \delta^d(x - y). \tag{5.62}$$

The right hand side has dimension $1/[x]^d$, so that also $\left[\frac{\delta}{\delta f(x)}\right] = 1/[x]^d$. Therefore, one is led to equate

$$\frac{\delta}{\delta f(x)} = \frac{1}{a^d} \frac{\delta}{\delta f(x')} \tag{5.63}$$

where $x' = x/a$ is the dimensionless length and a the lattice constant.

From the Euclidean action (2.34),

$$S_{\mathrm{E}} = \int \mathrm{d}^D x \mathrm{d}\tau \; - J a^{2-D} \frac{1}{2} (\partial_\mu^{\mathrm{ph}} \phi - \frac{e^*}{\hbar} A_\mu)^2. \tag{5.64}$$

the dimensionless action,

$$S_{\mathrm{E}}' = \int \mathrm{d}^D x' \mathrm{d}\tau' \; - \frac{Ja}{\hbar c_{\mathrm{ph}}} \frac{1}{2} (\partial_\mu' \phi - A_\mu')^2, \tag{5.65}$$

is obtained by the substitutions,

$$x = ax' \qquad \tau = \frac{a}{c_{\mathrm{ph}}} \tau' \qquad A_\mu = \frac{\hbar}{ae^*} A_\mu' \qquad S_{\mathrm{E}} = \hbar S_{\mathrm{E}}' \tag{5.66}$$

Now for the conductivity (5.43),

$$\omega_n \sigma_{ab}(\mathbf{k}, \mathrm{i}\omega_n) = \int \mathrm{d}(x - y) \mathrm{e}^{-\mathrm{i}k(x-y)} \frac{\hbar}{Z[0]} \frac{\delta}{\delta A_b(y)} \frac{\delta}{\delta A_a(x)} Z[A]\big|_{A=0}$$

$$= \frac{a^{D+1}}{c_{\mathrm{ph}}} \int \mathrm{d}(x' - y') \mathrm{e}^{-\mathrm{i}k'(x'-y')} \frac{\hbar}{Z[0]}$$

$$\left(\frac{c_{\mathrm{ph}}}{a^{D+1}}\right)^2 \left(\frac{ae^*}{\hbar}\right)^2 \frac{\delta}{\delta A_b'(y')} \frac{\delta}{\delta A_a'(x')} Z[A']\big|_{A'=0} \tag{5.67}$$

This expression is generally valid after the substitutions (5.66), not just for the superconductor action (5.65). Still, for the superconductor one finds,

$$\frac{\delta}{\delta A_b'(y')} \frac{\delta}{\delta A_a'(x')} Z[A'] = \frac{Ja}{\hbar c_{\mathrm{ph}}} \delta_{ab} \delta(x' - y') + \left(\frac{Ja}{\hbar c_{\mathrm{ph}}}\right)^2 \langle \partial_a' \phi(x') \partial_b' \phi(y') \rangle. \tag{5.68}$$

Following a procedure similar to (5.52), one finds the dimensionless version,

$$\langle \partial_a' \phi(x') \partial_b' \phi(y') \rangle = -\frac{\hbar c_{\mathrm{ph}}}{Ja} \int \mathrm{d}^{D+1} k' \mathrm{e}^{\mathrm{i}k'(x'-y')} \frac{k_a' k_b'}{k'^2}. \tag{5.69}$$

For the conductivity we then find,

$$\omega_n \sigma_{ab}(\mathbf{k}, i\omega_n) = \frac{c_{\mathrm{ph}}}{a^{D+1}} \hbar \frac{Ja}{\hbar c_{\mathrm{ph}}} \frac{e^{*2}a^2}{\hbar^2} [\delta_{ab} - \frac{k'_a k'_b}{k'^2}] = Ja^{2-D} \frac{e^{*2}}{\hbar^2} [\delta_{ab} - \frac{k_a k_b}{k^2}], \quad (5.70)$$

which agrees with (5.53), as in $D = 3$ we have $Ja^{2-D} = \hbar^2 \rho_s/m^*$. One can now proceed to real time just as in the previous section.

5.A.4 Bose-Mott insulator

The Bose-Mott insulator is a condensate of phase-vortices. One must express the phase field ϕ in terms of dual gauge fields which couple to a dual Higgs field. Across the phase transition, the action is (5.15),

$$S'_{\mathrm{E}} = \int d\tau' d^3 x' \frac{1}{2} g(\epsilon_{\mu\nu\kappa\lambda} \partial'_\nu b'_{\kappa\lambda})^2 + \frac{1}{2} |\Phi|^2 (\frac{1}{2} \sum_\alpha \delta_{\alpha\kappa} \partial'^{\mathrm{ph}}_\lambda \phi - b'_{\kappa\lambda})^2$$
$$+ \epsilon_{\mu\nu\kappa\lambda} \partial'_\nu b'_{\kappa\lambda} A'_\mu - \frac{1}{4\mu} (\partial'^c_\mu A'_\nu - \partial'^c_\nu A'_\mu)^2. \quad (5.71)$$

Again, since the conductivity is a property of the medium, we can leave out the (vacuum) Maxwell term. We can then directly integrate out the dual gauge fields, yielding an expression quadratic in the photon field, which can be inserted in Eq. (5.67). Now we run into the standard problem for calculating propagators for gauge fields: the gauge invariant inverse propagator in the Lagrangian cannot be inverted, in essence because it is a transversal projector, and no projector but the unit matrix has an inverse. The solution is to fix the gauge, most conveniently using the Lorenz gauge. We had already assumed this gauge fix in going to Eq. (5.15).

The action simplifies considerably. The only catch is that in the end result, one should remember to impose the constraints $\partial'_\mu w'_\mu = 0$ and $\partial'_\mu A'_\mu = 0$ by inserting the transversal projector $\delta_{\mu\nu} - k'_\mu k'_\nu/k'^2$ in the numerator. We denote with a ˜ components that are Lorenz-gauge fixed. Then

$$(\epsilon_{\mu\nu\kappa\lambda} \partial'_\nu b'_{\kappa\lambda})^2 = -b'_{\mu\lambda}(\partial'^2 \delta_{\mu\nu} - 2\partial'_\mu \partial'_\nu) b'_{\nu\lambda} \rightarrow -\tilde{b}'_{\kappa\lambda} \partial'^2 \tilde{b}'_{\kappa\lambda}. \quad (5.72)$$

Also the condensate mode $\partial'^{\mathrm{ph}}_\mu \chi$ does not couple to the dual gauge field b' and does therefore not contribute to the photon correlation function. The Higgs term is then simply $\frac{1}{2}|\Phi|^2(\tilde{b}'_{\kappa\lambda})^2$. We are now in a position to integrate out the

dual gauge field,

$$\int \mathrm{d}\tau' \mathrm{d}^3 x' \; -\frac{1}{2} g \tilde{b}'_{\kappa\lambda} \partial'^2 \tilde{b}'_{\kappa\lambda} + \frac{1}{2}|\Phi|^2 (\tilde{b}'_{\kappa\lambda})^2 + \epsilon_{\mu\nu\kappa\lambda} \partial'_\nu b'_{\kappa\lambda} A'_\mu$$

$$= \int \mathrm{d}\tau' \mathrm{d}^3 x' \; \frac{1}{2}\mathscr{G}^{-1} \tilde{b}'_{\kappa\lambda} [\tilde{b}'_{\kappa\lambda} + 2\mathscr{G}\epsilon_{\kappa\lambda\nu\mu} \partial'_\nu A'_\mu]$$

$$= \int \mathrm{d}\tau' \mathrm{d}^3 x' \; \frac{1}{2}\mathscr{G}^{-1} [\tilde{b}'_{\kappa\lambda} + \mathscr{G}\epsilon_{\kappa\lambda\nu\mu} \partial'_\nu A'_\mu]^2 - \frac{1}{2}\epsilon_{\kappa\lambda\nu\mu} \partial'_\nu A'_\mu \mathscr{G}\epsilon_{\kappa\lambda\sigma\rho} \partial'_\sigma A'_\rho$$

$$\rightarrow \int \mathrm{d}\tau' \mathrm{d}^3 x' \; \frac{1}{2} A'_\mu (\delta_{\mu\nu}\partial'^2 - \partial'_\mu \partial'_\nu)\mathscr{G} A'_\nu. \tag{5.73}$$

Here we have defined the inverse dual gauge field propagator $\mathscr{G}^{-1} = -g\partial'^2 + |\Phi|^2$. To calculate the correlation function, we should apply a Fourier transformation as in (5.48),

$$\int \mathrm{d}\tau' \mathrm{d}^3 x' \; \frac{1}{2} A'_\mu (\delta_{\mu\nu}\partial'^2 - \partial'_\mu \partial'_\nu)(-g\partial'^2 + |\Phi|^2)^{-1} A'_\nu =$$

$$\int \mathrm{d}^{D+1} k' \; -\frac{1}{2} A'_\mu(-k') \frac{\delta_{\mu\nu}k'^2 - k'_\mu k'_\nu}{gk'^2 + |\Phi|^2} A'_\nu(k'). \tag{5.74}$$

The conductivity is now obtained by inserting this in (5.67),

$$\omega_n \sigma_{ab}(\mathbf{k}, \mathrm{i}\omega_n) = \frac{\hbar c_{\mathrm{ph}}}{a^{D-1}} \frac{e^{*2}}{\hbar^2} \int \mathrm{d}^d(x'-y') \mathrm{e}^{-\mathrm{i}k'(x'-y')} \frac{1}{Z[0]} \frac{\delta}{\delta A'_b(y')} \frac{\delta}{\delta A'_a(x')} Z[A']$$

$$= \frac{\hbar c_{\mathrm{ph}}}{a^{D-1}} \frac{e^{*2}}{\hbar^2} \int \mathrm{d}^d(x'-y') \mathrm{d}\bar{k}' \; \mathrm{e}^{-\mathrm{i}(k'+\bar{k}')(x'-y')} \frac{\delta_{ab}\bar{k}'^2 - \bar{k}'_a \bar{k}'_b}{g\bar{k}'^2 + |\Phi|^2}$$

$$= \frac{1}{g} \frac{\hbar c_{\mathrm{ph}}}{a^{D-1}} \frac{e^{*2}}{\hbar^2} \frac{\delta_{ab}k'^2 - k'_a k'_b}{k'^2 + |\Phi|^2/g} = \frac{e^{*2}\rho_{\mathrm{s}}}{m^*} \frac{\delta_{ab}k^2 - k_a k_b}{k^2 + |\Phi|^2/ga^2} \tag{5.75}$$

In the last step we reverted to dimensionful units. In the limit $|\Phi|^2 \to 0$ this reduces to the result for the superconductor (5.70). We are interested in the DC and AC conductivity, and therefore take the limit $\mathbf{k} \to 0$, to find,

$$\sigma_{ab}(\mathrm{i}\omega_n) = \frac{e^{*2}\rho_{\mathrm{s}}}{m^*} \frac{1}{\omega_n} \frac{\delta_{ab}\omega_n^2}{\omega_n^2 + c_{\mathrm{ph}}^2 |\Phi|^2/ga^2} \equiv \frac{e^{*2}\rho_{\mathrm{s}}}{m^*} \delta_{ab} \frac{\omega_n}{\omega_n^2 + M^2}. \tag{5.76}$$

Here we defined $M^2 = \frac{c_{\mathrm{ph}}^2}{a^2} \frac{|\Phi|^2}{g}$. We continue to real time by $\mathrm{i}\omega_n \to \omega + \mathrm{i}\eta$, where $\eta > 0$. Then,

$$\sigma_{ab}(\omega) = \frac{e^{*2}\rho_{\mathrm{s}}}{m^*} \delta_{ab} \frac{-\mathrm{i}\omega}{-\omega^2 - 2\mathrm{i}\omega\eta + M^2}$$

$$= \frac{e^{*2}\rho_{\mathrm{s}}}{m^*} \delta_{ab} \frac{-\mathrm{i}\omega}{\big((\omega - M) + \mathrm{i}\eta\big)\big((-\omega - M) + \mathrm{i}\eta\big)}. \tag{5.77}$$

Clearly there are poles at $\omega = M - i\eta$ and $\omega = -M + i\eta$. Using the Sokhostsky formula Eq. (5.54) for the pole near $\omega = M$ we find for the real part of the conductivity,

$$\operatorname{Re}\sigma_{ab}(\omega) = Ja^{2-D}\frac{e^{*2}}{\hbar^2}\delta_{ab}\frac{-i\omega}{-\omega-M}\left(-i\pi\delta(\omega-M)\right) = Ja^{2-D}\frac{e^{*2}}{\hbar^2}\delta_{ab}\frac{\pi}{2}\delta(\omega-M).$$

$$(5.78)$$

We can conclude that there are gapped poles at $\omega = \pm M = \pm\frac{c_{\text{ph}}}{a}\sqrt{|\Phi|^2/g}$, and the pole strength of each is half of that of the superconductor [cf. Eq (5.56)].